Internal Wave-Wave Resonance Theory: Fundamentals and Limitations

Eric Hirst
Applied Physics Laboratory
University of Washington
Mailstop HN 10
Seattle, Wa. 98115

ABSTRACT

First, two terms of a resonant transfer integral are derived for a simple one-dimensional analog to the equations of fluid motion. The purpose of this rather academic exercise is to more clearly illustrate the assumptions of the resonant interaction approximation. Second, it is shown that, in much of the region of phase space where nonlinear interactions are usually considered weak enough for the theory to be applicable, nonlinear transfers due to bottom scattering and other mechanisms cannot be ignored.

INTRODUCTION

Weakly nonlinear resonant interactions have been studied extensively as a model for predicting the temporal evolution of various broad-band wave spectra. Hasselmann (1962, 1966) derived a general wave-wave resonance theory, which I will refer to as the resonant interaction approximation (RIA). RIA has been used with some success on the surface wave interaction problem (WAMDI, 1988), but it is still unclear how applicable it is to internal waves. RIA-based internal wave spectral evolution equations were derived and evaluated by Olbers (1976), McComas and Bretherton (1977, henceforth MB), and Pomphrey, et al. (1980). Results of these calculations have yet to be verified for any realistic ocean internal wave field, however, and the validity of RIA for large portions of the internal wave spectrum has been called into question by Holloway (1980, 1982), Henyey et al. (1986), and Müller, et al. (1986).

The initial portion of this paper will attempt to highlight some of the basic points of an RIA derivation using a 1-D analog. The somewhat ad hoc derivation will follow Hasselmann (1966); a more careful derivation using the method of multiple time scales is given by Benney and Saffman (1966), who also begin with a one dimensional example for readability. It must be stressed that, since RIA reduces the dimension of any problem by one, the resonant "surface" for this example will just be a set of three points. The purpose of this exercise is strictly to clarify the mechanics of an RIA derivation, and not to offer a new way of solving one dimensional problems.

In the past, criticisms of RIA have focused on mapping out regions of phase space where RIA predicts interactions so strong that they violate the theory's assumptions of "weakness." There are regions of phase space, however, where RIA predicts interactions which are so weak that they will be overshadowed by other nonlinear mechanisms, most notably bottom scattering. The second portion of this paper attempts to map the regions in wavenumber and frequency space where resonant interaction theory either violates its own assumptions or predicts interactions so weak that they will be overshadowed by other mechanisms.

DERIVATION OF A SPECTRAL EVOLUTION EQUATION

Derivation of a resonant spectral evolution equation directly from the equations of fluid motion is, among other things, a monumental exercise in algebra. Fortunately, the critical steps may be highlighted by deriving a similar evolution equation for a one dimensional analog. The somewhat modified Korteveg-DeVries (KdV) equation,

$$\frac{\partial \phi}{\partial t} + \frac{\partial^3 \phi}{\partial x^3} + \varepsilon \phi \frac{\partial \phi}{\partial x} = 0, \tag{1}$$

has many of the same basic properties as the equations of fluid motion. It is first order in time, non-dissipative, dispersive, and contains a quadratic nonlinearity. The dependent variable $\phi(x,t)$ is assumed to be of order one, and ε is a small parameter, analogous to a Rossby number for low frequency internal waves.

The first step in our streamlined derivation will be to expand (1) in a Fourier series. If we assume a periodic solution in a domain $-L \le x \le L$, we may write

$$\phi(x,t) = \sum_n \hat{\phi}(n,t) e^{\frac{in\pi x}{L}}, \tag{2}$$

where the summation is over all integer mode numbers, and

$$\hat{\phi}(n,t) = \frac{1}{2L} \int_{-L}^{L} dx \, \phi(x,t) e^{\frac{-in\pi x}{L}}. \tag{3}$$

To handle the nonlinear term, we make use of the convolution rule,

$$\frac{1}{2L} \int_{-L}^{L} dx \, f(x,t) g(x,t) e^{\frac{-in\pi x}{L}} = \sum_{n_1} \sum \hat{f}(n_1,t) \hat{g}(n_2,t) \delta_{n, n_1+n_2}, \tag{4}$$

where δ_{n, n_1+n_2} is the Kronecker delta. The KdV equation may then be written

$$\frac{\partial \hat{\phi}}{\partial t} - ik^3 \hat{\phi} = \frac{-ik\varepsilon}{2} \sum_{n_1} \sum \delta_{n, n_1+n_2} \hat{\phi}_1 \hat{\phi}_2, \tag{5}$$

where $k = n\pi/L$ is the wavenumber, and $\hat{\phi}_j \equiv \hat{\phi}(n_j,t)$. Note that the factor $k/2 = (n_1+n_2)\pi/2L$ appears due to the Kronecker delta and the symmetry of the summation.

It would be possible to find a numerical scheme to evaluate (5) directly for a finite number of modes. The convolution sum could be handled by a fast Fourier transform algorithm, and a suitable procedure could be used to integrate in time. This technique is simply a pseudo-spectral

Fourier-Galerkin scheme, however, and has the same basic strengths and weaknesses as any of the competing numerical methods. To take advantage of the supposed weakness of the nonlinear term, we instead make a perturbation expansion about a first order linear solution.

Expanding our solution in powers of ε, we may write

$$\hat{\phi} = {}_1\hat{\phi} + {}_2\hat{\phi}\varepsilon + {}_3\hat{\phi}\varepsilon^2 + \cdots, \tag{6}$$

where ${}_j\hat{\phi} = O(1)$. The linear solution is then

$${}_1\hat{\phi} = A(n,t=0)e^{i\omega t}, \tag{7}$$

where $\omega \equiv k^3$ is the intrinsic frequency, and the time t is measured from the most recent time the spectrum was measured or calculated. The $A(n,0)$'s are chosen such that ${}_1\hat{\phi} = A = \hat{\phi}$ at $t = 0$. The second order solution will then be obtained from

$$\frac{\partial {}_2\hat{\phi}}{\partial t} - i\omega\, {}_2\hat{\phi} = \frac{-ik}{2}\sum_{n_1}\sum_{n_2}\delta_{k,k_1+k_2}A_1A_2e^{i(\omega_1+\omega_2)t}, \tag{8}$$

where the subscripts on amplitudes A_j and frequencies ω_j denote dependence on mode number $n_j = Lk_j/\pi$. (Unsubscripted forms will generally be dependent on mode number n.)

Equation (8) has the solution

$${}_2\hat{\phi} = \frac{-ik}{2}e^{i\omega t}\int_0^t d\tau \sum_{n_1}\sum_{n_2}\delta_{k,k_1+k_2}A_1A_2e^{i(\omega_1+\omega_2-\omega)\tau}. \tag{9}$$

This may be integrated in τ to obtain

$${}_2\hat{\phi} = \frac{-ik}{2}e^{i\omega t}\sum_{n_1}\sum_{n_2}\delta_{k,k_1+k_2}A_1A_2\Delta(\Omega,t), \tag{10}$$

where $\Omega \equiv \omega_1+\omega_2-\omega$, and

$$\Delta(\Omega,t) \equiv \frac{e^{i\Omega t}-1}{i\Omega}. \tag{11}$$

A similar but slightly more complicated expression may be obtained for ${}_3\phi$. While the third order quantities must be included in the full resonant transfer equation for both KdV and internal wave systems, they will be ignored in this discussion.

At this point, we should make some observations on just what "linear solution" we are expanding about. Recall that the purpose of RIA is to predict the temporal evolution of a given spectrum. Presumably at $t = 0$, we know the spectrum and the $A(N)$'s are chosen such that the first older solution ${}_1\phi$ is the complete solution ϕ. It is clear from (9) that ${}_2\phi = 0$ at $t = 0$; the same applies to higher order terms. But for larger times, the spectrum will evolve, and the $A(k)$'s will periodically have to be updated (and t reset to zero in my notation) for the series (6) to correctly approximate the true solution.

In an actual RIA calculation, phase information is sacrificed and $A(k)$ is not actually calculated. Instead we look for an equation governing the temporal evolution of an action density $a(k,t)$, defined as

$$\begin{aligned} a(k,t) &\equiv \frac{1}{\omega}\langle\hat{\phi}\hat{\phi}^*\rangle \\ &= \frac{1}{\omega}\langle{}_1\hat{\phi}_1\hat{\phi}^*\rangle \\ &+ \frac{\varepsilon}{\omega}\left\{\langle{}_1\hat{\phi}_2\hat{\phi}^*\rangle + \langle{}_2\hat{\phi}_1\hat{\phi}^*\rangle\right\} \\ &+ \frac{\varepsilon^2}{\omega}\left\{\langle{}_1\hat{\phi}_3\hat{\phi}^*\rangle + \langle{}_2\hat{\phi}_2\hat{\phi}^*\rangle + \langle{}_3\hat{\phi}_1\hat{\phi}^*\rangle\right\} + \cdots, \end{aligned} \tag{12}$$

where the brackets represent ensemble averages and asterices indicate complex conjugates. Our choice of first order solution ${}_1\phi$ implies that the lowest (second) order action term $\omega^{-1}\langle{}_1\hat{\phi}_1\hat{\phi}^*\rangle$ will be constant. If we can assume that all amplitudes $A(k)$ are uncorrelated and Gaussian, then the third order terms, with their associated triple correlations, vanish identically. It must be recognized that strong interactions in even an initially Gaussian wave field might set up correlations between interacting wave modes. In this case, the third order (cumulant) terms may not be neglected, and the theory will fail. If our Gaussian assumption is valid, we have

$$\frac{\partial a}{\partial t} = \frac{\partial}{\partial t}\frac{\varepsilon^2}{\omega}\left\{\langle{}_1\hat{\phi}_3\hat{\phi}^*\rangle + \langle{}_2\hat{\phi}_2\hat{\phi}^*\rangle + \langle{}_3\hat{\phi}_1\hat{\phi}^*\rangle\right\} + \cdots. \tag{13}$$

To perform the averaging on the middle term, it is useful to first write equation (10) as a single sum without a Kronecker delta.

$${}_2\hat{\phi} = \frac{-ik}{2}e^{i\omega t}\sum_{n_1} A(n_1)A(n-n_1)\Delta_1, \tag{14}$$

where $\Delta_j \equiv \Delta(\omega(k_j)+\omega(k-k_j)-\omega,t)$. We then have

$$\langle{}_2\hat{\phi}_2\hat{\phi}^*\rangle = \frac{k^2}{4}\sum_{n_1}\sum_{n_2}\langle A(n_1)A(n-n_1)A^*(n_2)A^*(n-n_2)\rangle\Delta_1\Delta_2^*. \tag{15}$$

Again assuming that the A's are Gaussian random variables, we split up the fourth order moment into second order moments to obtain

$$<_2\hat{\phi}_2\hat{\phi}^*> = \frac{k^2}{4}\sum_{n_1}\sum_{n_2}\Big\{<A(n_1)A(n-n_1)><A^*(n_2)A^*(n-n_2)> + <A(n_1)A^*(n-n_2)><A(n-n_1)A^*(n_2)> + <A(n_1)A^*(n_2)><A(n-n_1)A^*(n-n_2)>\Big\}\Delta_1\Delta_2^*. \tag{16}$$

Because $<A(n_1)A(n_2)>$ vanishes for $n_1 \neq -n_2$ ($A^*(n)=A(-n)$), each of the second order moments in the first term vanishes for $n \neq 0$. Because of the k^2 factor in front of the integral, we may then drop this term.

The second term vanishes except when $n_1 + n_2 = n$. If we replace the summation variable n_2 with n_2+n, we find that the third term vanishes except when $n = n_1 - n_2$. We may then insert and make use of two new Kronecker deltas to write

$$<_2\hat{\phi}_2\hat{\phi}^*> = \frac{k^2}{4}\sum_{n_1}\sum_{n_2}\delta_{k,k_1+k_2}|\Delta(\omega_1+\omega_2-\omega,t)|^2 a_1 a_2 \omega_1\omega_2 + \delta_{k,k_1-k_2}|\Delta(\omega_1-\omega_2-\omega,t)|^2 a_1 a_2 \omega_1\omega_2. \tag{17}$$

Here we have made the substitution

$$a(n,t) \approx \frac{1}{\omega}<_1\hat{\phi}_1\hat{\phi}^*> = \frac{1}{\omega}<A(n)A^*(n)>, \tag{18}$$

valid for short amounts of time since the most recent update to the spectrum. The amount of time for which this is valid will be inversely proportional to the strength of the interactions.

The spectral evolution equation for $a(k)$ will be of the form

$$\frac{\partial a}{\partial t} \approx \frac{\varepsilon^2}{\omega}\frac{\partial}{\partial t}<_2\hat{\phi}_2\hat{\phi}^*>, \tag{19}$$

where again the (non-negligible) $<_1\hat{\phi}_3\hat{\phi}>$ terms have been dropped for simplicity. The time derivative acts only on the $|\Delta|^2$ functions on the right hand side of (17), which have the explicit form

$$|\Delta(\Omega,t)|^2 = \frac{2-2\cos(\Omega t)}{\Omega^2}. \tag{20}$$

The limiting behavior of these functions is essential to the validity of RIA theory. We find a short time limit of

$$\lim_{t\to 0}\left[|\Delta(\Omega,t)|^2\right] = t^2, \tag{21}$$

and a long time limit of

$$\lim_{t\to\infty}\left[|\Delta(\Omega,t)|^2\right] = 2\pi t\,\delta(\Omega), \tag{22}$$

where $\delta(\Omega)$ is now a Dirac delta. For intermediate values of t, we find a sinc-like function in Ω with a bandwidth $\approx 2\pi/t$, as shown in Figure1. The value of t chosen for this function must be of the same or lesser order than the amount of time our expansion (12) remains accurate and rapidly convergent, such that (18) remains valid.

RIA theory chooses to take the long time limit (22) as an approximation of $|\Delta|^2$. In doing so, it assumes that the first order solution holds steady long enough for the bandwidth of the function in Figure1 to become small in comparison with a characteristic bandwidth in the internal wave frequency spectrum. By "characteristic bandwidth," I mean a bandwidth over which amplitudes

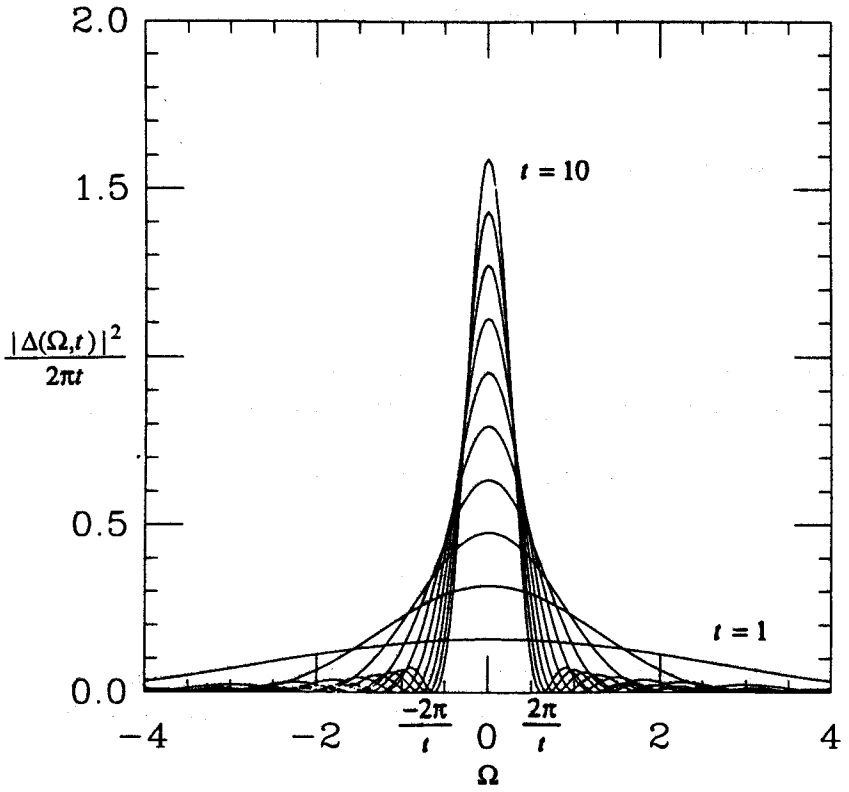

Figure 1. The function $|\Delta|^2/2\pi t$, approximated as a Dirac delta in RIA theory.

vary essentially linearly, such that the filter function depicted in figure 1 may be safely replaced by a Dirac delta. This bandwidth has traditionally been taken as the period of the wave n, yielding the validity criterion

$$\frac{2\pi\nu}{\omega} < 1, \tag{23}$$

where ν^{-1} is the interaction time over which (18) remains valid. It must be stressed that (23) is a necessary but not sufficient criterion for RIA's validity -- we must also be able to somehow justify dropping the cumulant term in (12). However, (23) is an easy test to perform, and Holloway's (1980) implementation of it is still the only quantitative attempt to establish a high wavenumber cutoff for RIA.

Applying (22), we obtain

$$\frac{\partial a}{\partial t} \approx \frac{\pi k^2\varepsilon^2}{2\omega}\sum_{n_1}\sum_{n_2}\delta_{n,n_1+n_2}\delta(\omega_1+\omega_2-\omega)a_1a_2\omega_1\omega_2 \tag{24}$$
$$+\,\delta_{n,n_1-n_2}\delta(\omega_1-\omega_2-\omega)a_1a_2\omega_1\omega_2,$$

plus similar forms for the $<_1\hat{\phi}_3\hat{\phi}>$ terms. In the limit of a continuous spectrum, we have

$$\frac{\partial a}{\partial t} \approx \frac{\pi k^2\varepsilon^2}{2\omega}\int_{-\infty}^{\infty}\int_{-\infty}^{\infty}dk_1dk_2\delta(k-k_1-k_2)\delta(\omega_1+\omega_2-\omega)a_1a_2\omega_1\omega_2 \tag{25}$$
$$+\,\delta(k-k_1+k_2)\delta(\omega_1-\omega_2-\omega)a_1a_2\omega_1\omega_2.$$

Notice that RIA has reduced the dimension of the problem by one. Equation (25) is now a zero-dimensional integral(!); the corresponding equation for internal waves will be two-dimensional.

The transfer integral for internal waves takes the form (Müller, et al, 1986)

$$\frac{\partial a}{\partial t} = \int_{-\infty}^{\infty}\int_{-\infty}^{\infty}d\mathbf{k}_1d\mathbf{k}_2T^+\delta(\mathbf{k}-\mathbf{k}_1-\mathbf{k}_2)\delta(\omega_1+\omega_2-\omega)(a_1a_2-aa_1-aa_2) \tag{26}$$
$$+\,2T^-\delta(\mathbf{k}-\mathbf{k}_1+\mathbf{k}_2)\delta(\omega_1-\omega_2-\omega)(a_1a_2+aa_1-aa_2),$$

where a is the internal wave action density and T^+ and T^- are rather messy coupling coefficients depending on the wave vectors $\mathbf{k}$, $\mathbf{k}_1$, and $\mathbf{k}_2$. Resonant interactions, then, are confined to "triads" of three waves satisfying the conditions $\mathbf{k}=\mathbf{k}_1\pm\mathbf{k}_2$ and $\omega=\omega_1\pm\omega_2$.

The appeal of RIA theory is perhaps chiefly tied to the reduction in dimensions associated with the δ functions acting on the frequencies. However, the validity of this δ function is by no means assured, as suggested by the requirement (23). Additionally, the Gaussian assumption, which allowed us to drop the cumulants in (12), suggests another restriction on the strength of the interactions, namely that the "forcing" waves n_1 and n_2 must have rapid decorrelation times

compared to the interaction rates. This restriction is discussed briefly in Müller et al. (1986), in the context of their equation (70), but imposes a criterion which has been relatively difficult to quantify.

For very weak interactions, we may expect the perturbation expansion to be a useful model. However, it will be pointed out in the latter section of this paper that when resonant interactions become too weak, other nonlinear transfer mechanisms must also be considered.

VALIDITY AND APPLICABILITY OF RESONANCE THEORY

In the tradition of Holloway (1980), interaction times predicted by McComas (1977), and MB were compared with other readily available characteristic time scales. Approximate formulas for induced diffusion (ID) and parametric subharmonic instability (PSI) time scales, given by McComas and Müller (1981, henceforth MM), were applied to the GM76 (Cairns and Williams, 1976) model spectrum. The model spectrum and the resulting time scales are shown in Figures 2 and 3, respectively. Numerical values for the GM76 spectrum were inertial frequency $f = 7.0\times10^{-5}\text{s}^{-1}$, buoyancy frequency $N = 71f$, stratification scale $b = 1300\text{m}$, peak mode number $j^* = 3$, and dimensionless energy scale $E = 6.3\times10^{-5}$. The hydrostatic dispersion relation

$$\omega = \sqrt{f^2 + N^2 \frac{k_h^2}{k_z^2}}, \tag{27}$$

where k_h and k_z are the horizontal and vertical wave numbers, was used throughout.

Figure 3 is essentially an attempt to replicate figure 4 of McComas (1977) and figure 11 of MB, without solving the full transfer integral (26). It was generated using equations (11) and (22) of MM, with the ID equation (11) applying for frequencies $\omega > 2f$, and the PSI equation (22) applying for $\omega < 2f$. A value of $x = 1$, or $\omega' = 2.5f$, was chosen in MM's equation (22) to better fit the PSI time scales indicated by McComas (1977) and MB. (The transfer times in figure 8 of MM appear to be approximately ten times too high.)

The figures compare reasonably well, except at very low wave numbers, and at the region near $\omega = 2f$, where interaction rates pass through zero in the earlier plots. The discrepancies at low wave numbers do not substantially affect the results which will follow. Also, there is no reason to expect the actual *strength* of the interactions to become small near $\omega = 2f$. The rightward leaning "spikes" which appear in the earlier plots have therefore been truncated.

Mean Free Paths and Bottom Scattering

Horizontal and vertical "mean free paths," MFP_h and MFP_z of resonantly interacting internal waves, plotted in Figures 4 and 5, were then calculated by multiplying the resonant interaction times in Figure 3 with the horizontal and vertical group velocities. The mean free paths then correspond to the distances which waves may be expected to propagate before they are significantly altered by resonant interactions. If a wave propagates more than one ocean depth in the vertical (or one ocean width in the horizontal) before it has time to resonantly interact, it

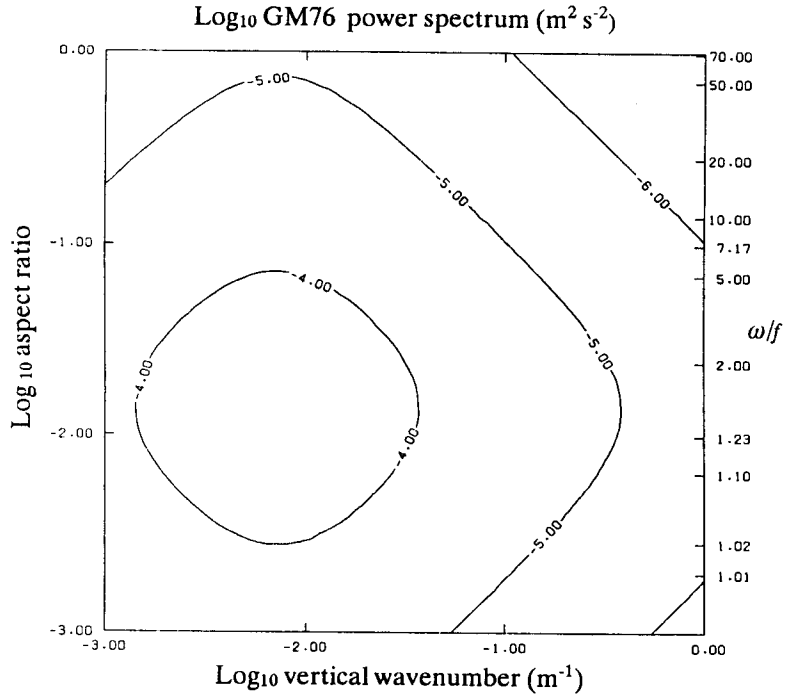

Figure 2. The GM76 model spectrum. The energy density is multiplied by the vertical wavenumber k_z and the aspect ratio α, such that the quantity plotted integrated over the area $d\log(k_z)d\log(\alpha)$ gives the energy in that area.

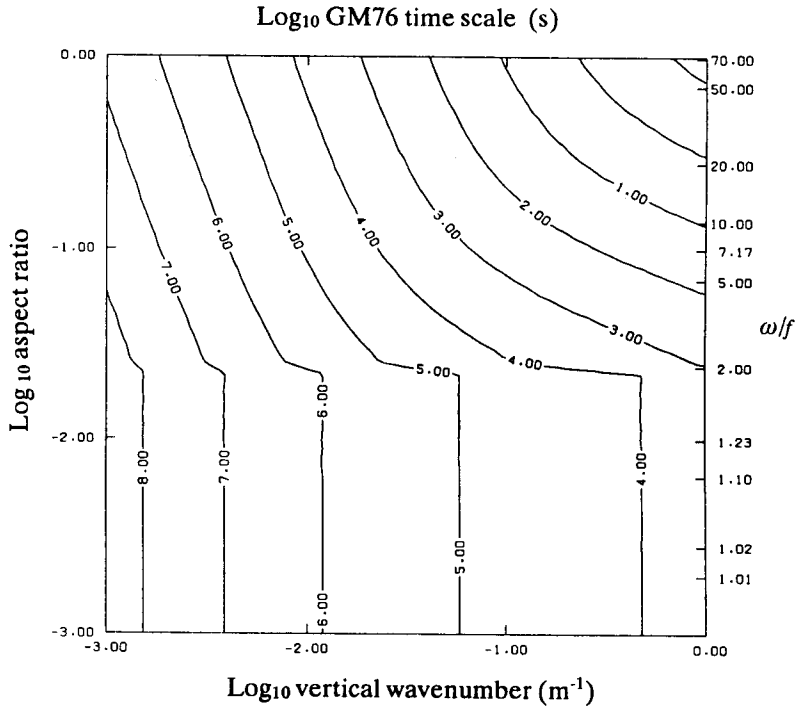

Figure 3. Interaction time scales predicted by RIA theory. The formulas of McComas and Müller (1981) are used to approximate values previously obtained by solving the full RIA transfer integral.

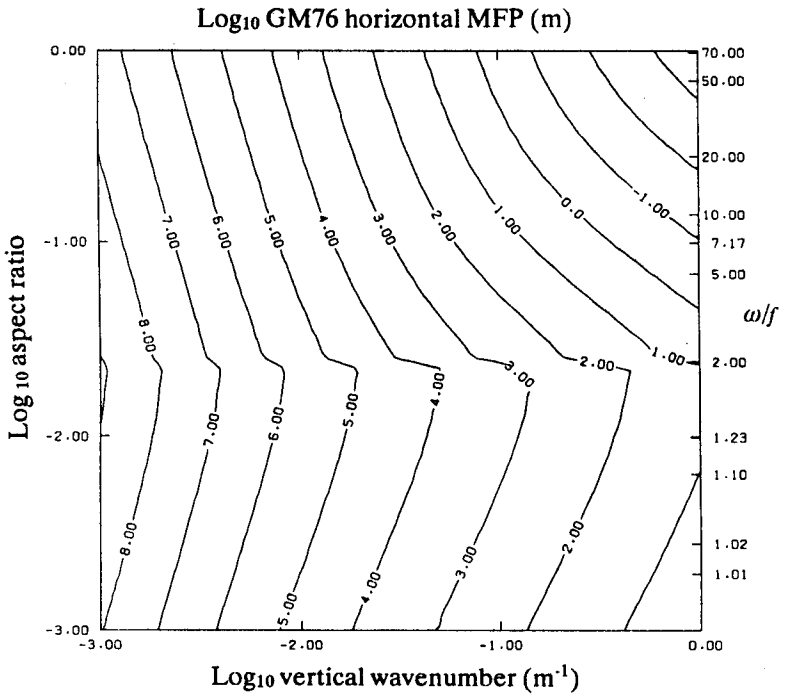

Figure 4. Horizontal "mean free paths" of resonantly interacting waves. In an infinite ocean, waves would be expected to propagate the distances shown before being consumed by resonant interactions. The quantity plotted is the product of the horizontal group velocity with the time scale of Figure 3.

cannot be well modeled without considering scattering effects. Figure 4 suggests that a substantial range of low wavenumber waves will be affected by bottom scattering.

Critical Layers

Two types of critical trapping may occur for low frequency waves, as schematically illustrated by Kunze and Müller (1989) in their figures 1A and 1B.

In the presence of variable baroclinic vorticity ζ, internal waves will experience an effective inertial frequency

$$f_{eff} = f + \frac{\zeta}{2}. \tag{28}$$

As a near-inertial wave propagates into a region in which f_{eff} exceeds the intrinsic frequency, its vertical group velocity will go to zero, sending its vertical wavenumber to infinity. This type of critical layer is discussed in detail in Kunze (1985). If we assume that f_{eff} varies linearly with depth as $|df_{eff}/dz| = 1.2f/3000s^{-1}m^{-1}$, where 3000m is the bottom depth, the change in f_{eff} which a wave may experience as it propagates may be estimated by

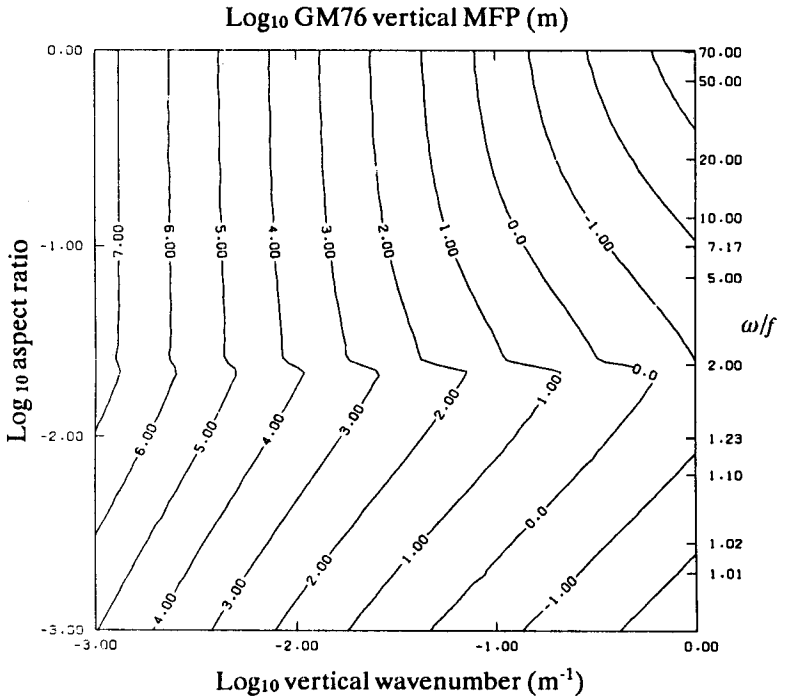

Figure 5. Vertical "mean free paths" of resonantly interacting waves. The quantity plotted is the product of the vertical group velocity with the time scale of Figure 3.

$$|\Delta f_{eff}| = \frac{1.2f}{3000\text{m}} \cdot \min(MFP_z, 3000\text{m}). \tag{29}$$

When $|\Delta f_{eff}| > \omega - f$, a wave may reach a critical layer of this type. An appropriate stall criterion will then be

$$\gamma > 1, \tag{30}$$

where $\gamma \equiv |\Delta f_{eff}|/(\omega - f)$ is plotted in Figure 6. It is seen that, for the parameters chosen, such critical layers may be experienced by waves with frequencies less than $1.2f$ and vertical wavelengths greater than approximately 300 meters.

A second type of critical layer may occur even when the effective Coriolis parameter is constant. A wave may have its intrinsic frequency shifted to f (or f_{eff}) by spatial variability in the geostrophic current. In a time independent mean flow U, the Eulerian frequency ω will be a constant along a ray path, while the intrinsic frequency will be given by $\omega_0 = \omega - \mathbf{k}\cdot\mathbf{U}$. Thus an appropriately oriented change of geostrophic current $\Delta U = \Delta U_{crit} \equiv (\omega - f)/k_h$ along a ray path will push the intrinsic frequency to f and cause the wave to stall. This type of critical layer is discussed in more detail by Olbers (1981).

ΔU_{crit} is plotted in Figure 7; Kunze and Müller (1989) suggest that critical layers are likely when

$$\Delta U_{crit} < 0.05\text{ms}^{-1}. \tag{31}$$

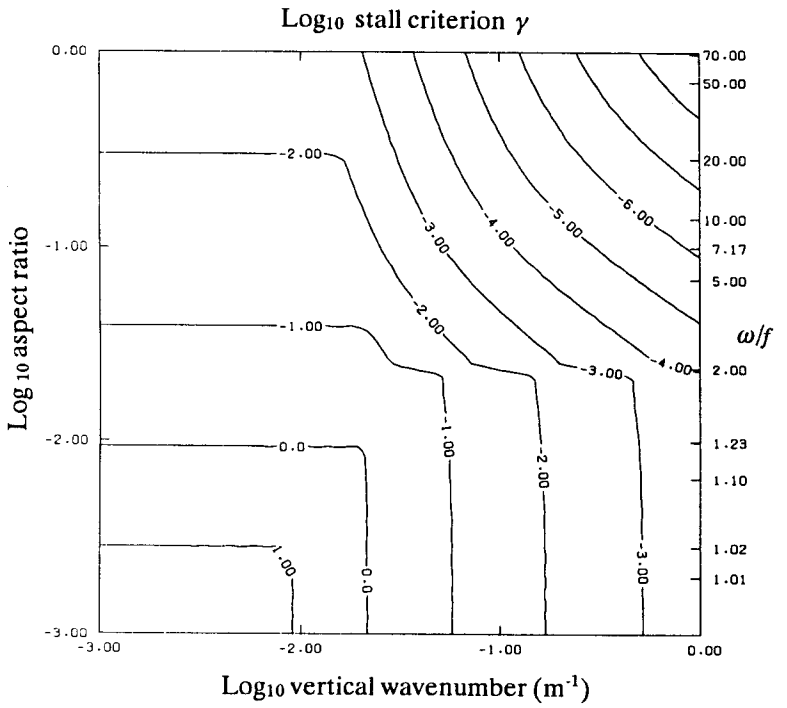

Figure 6. The stall criterion $\gamma = |\Delta f_{eff}|/(\omega - f)$. For $\gamma > 1$, the effective Coriolis frequency may increase to the wave frequency along a ray path, causing critical trapping.

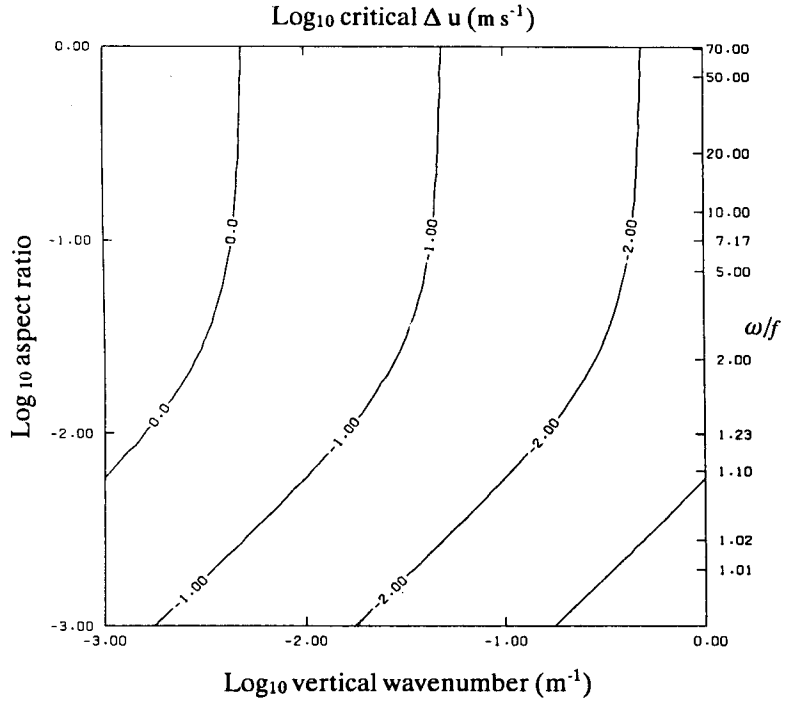

Figure 7. The change in the mean current along a ray path which, if appropriately oriented, will push a wave's intrinsic frequency below the inertial frequency, causing critical trapping.

The likelihood of a wave ever reaching such a critical layer will also depend strongly on that wave's mean free path, however. To account for this, we first define a Richardson number as

$$Ri \equiv \left[\frac{N \min(3000\text{m}, MFP_z)}{\Delta U}\right]^2. \tag{32}$$

Replacing ΔU with ΔU_{crit} gives a "critical Richardson number" of

$$Ri_{crit} \equiv \left[\frac{Nk_z \min(3000\text{m}, MFP_z)}{\omega - f}\right]^2, \tag{33}$$

which is plotted in Figure 8. We may supplement (31) by requiring that the shear be strong enough along a wave's mean free path for

$$Ri < Ri_{crit} \tag{34}$$

to hold. Since Kelvin-Helmholtz instability will occur when $Ri \leq 1/4$, we may conclude that the region in which this type of critical layer may occur will be bounded by the contours

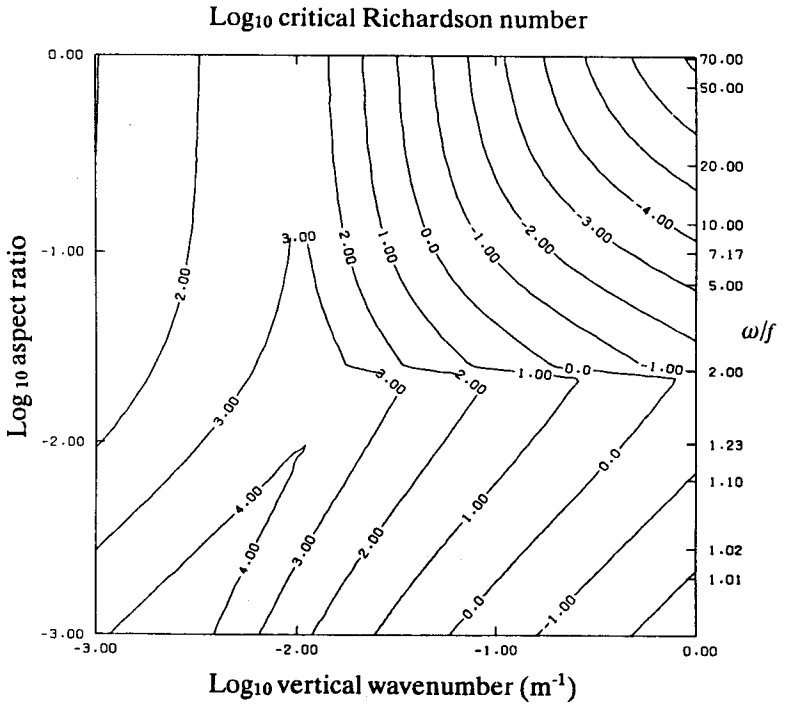

Figure 8. The critical Richardson number, on a scale of either the vertical mean free path or the ocean depth, required to cause trapping. If the actual Richardson number is greater than that shown, the shear will be too weak for this effect to occur in the vertical distance the wave can propagate before it is consumed by resonant interactions..

$\Delta U_{crit} = 0.05 ms^{-1}$ in figure 7 and $Ri_{crit} = 0.25$ in Figure 8.

It should be noted that the first phenomenon, in which $f_{eff} \rightarrow \omega$ along a ray path, is vertically anisotropic and may not occur among both upward and downward propagating waves simultaneously. The second phenomenon, in which ω_0 is shifted to f along a ray path, is strongly dependent on the orientation of the horizontal wave vector, which must be aligned with the mean flow. Finally, both of the critical layers described will no doubt be highly intermittent, and their importance in the overall spectral energy transfer is still unknown.

Validity regions

Figure 9 divides the internal wave spectrum into five sections, using information from Figures 5-9 and the various cutoff criteria listed in the text and in equations (23),(30), and (31). We first consider the three non-overlapping sections, divided by the solid lines. In the leftmost section, the vertical mean free path exceeds the canonical 3000 meter ocean depth, and we expect bottom reflection effects to be significant. This region also roughly corresponds to the region in which the horizontal mean free path is greater than 100 to 1000 kilometers, as indicated in Figure 4. In the rightmost section, which corresponds to the shaded portion of Holloway's (1980) figure 1a,

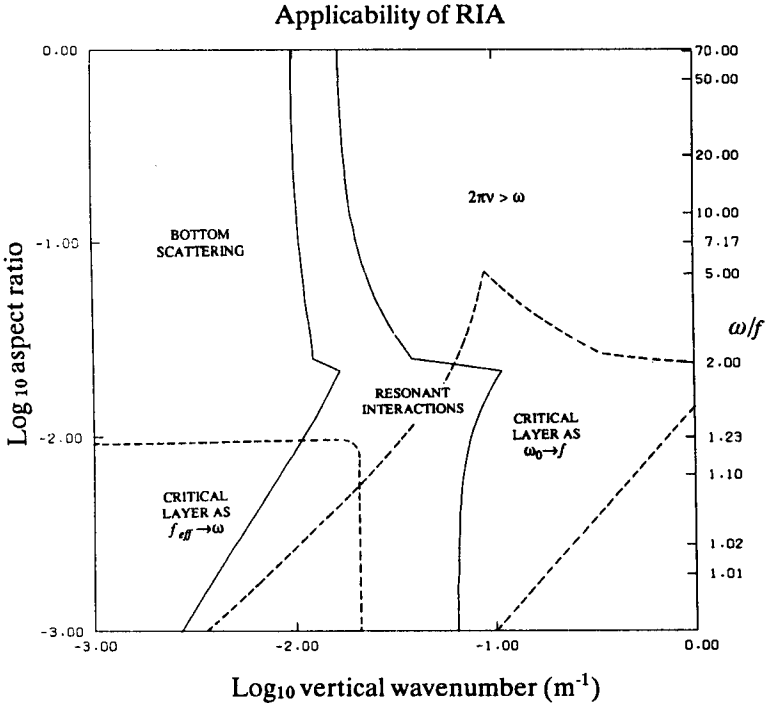

Figure 9. Map of RIA's potential applicability. In the rightmost solid region, the interaction time is less than one wave period, and we expect the perturbation expansion to fail. In the leftmost solid region, bottom reflections will be significant. In the center solid region, RIA may be useful. In the two dashed regions, the types of critical trapping discussed in the text may also be important.

the interaction time exceeds the wave period, and we expect the perturbation expansion to break down. (Again, this cutoff is a crude one, as equation (23) is not a sufficient condition for RIA's validity.)

In the center region, RIA may in fact prove useful. Several possible obstacles must still be recognized here, however. First, the Gaussian or random phase assumption must be tested to see if cumulants may in fact be ignored. Second, we see that much of this region is overlapped by the regions in which the two critical layer phenomena may (or may not) be significant, as indicated by the dashed curves.

The area inside the leftmost dashed region, based on the criterion (30), corresponds to waves which may be susceptible to the first type of critical layer discussed, in which $f_{eff} \rightarrow \omega$ along a ray path. The area inside the rightmost dashed region, bounded on the left by the curve $\Delta U_{crit} = 0.05\text{ms}^{-1}$ and on the right and top by the curve $Ri_{crit} = 0.25$, corresponds to waves which may be susceptible to the second type of critical layer, in which $\omega_0 \rightarrow f$. Since the dashed regions overlap much of RIA's "applicability region," one might be tempted to abandon the RIA theory altogether at this point. However, it should be mentioned that RIA's parametric subharmonic instability mechanism yields an energy flux toward the near-inertial portion of the spectrum (cf. MB); we may (boldly and blindly) speculate that this flux is in perfect balance with critical layer dissipation.

SUMMARY

The one-dimensional analog has made resonance theory somewhat more accessible to all who might be interested. Also, it has been pointed out that there is a rather substantial region in phase space where bottom reflections may dominate the nonlinear transfer. Finally, two types of critical trapping mechanisms have been discussed for near-inertial waves. While the net contribution by these mechanisms to the overall nonlinear transfer is unknown, it has been shown that they may affect waves over large regions of phase space, including much of the region where resonant interactions may occur. Since RIA does not predict equilibrium for near-inertial waves, however, it has been suggested that critical layer interactions may in fact complement RIA theory in this region.

ACKNOWLEDGMENTS

I would like to thank Peter Müller for his indispensable guidance and suggestions. I would also like to thank Terry Ewart, Jim Riley, and Eric D'Asaro for their feedback and support, and Eric Kunze for taking time to discuss critical layers with me. This work was supported by discretionary funds at the Applied Physics Laboratory at the University of Washington.

REFERENCES

Benney, D. J., and P. G. Saffman, 1966: Nonlinear interactions of random waves in a dispersive medium, *Proc. Roy. Soc., Ser. A, 289*, 301-320

Cairns, J. L., and G. O. Williams, 1976: Internal wave observations from an internal float, 2, *J. Geophys. Res., 81*, 1943-1960.

Hasselmann, K., 1962: On the non-linear energy transfer in a gravity-wave spectrum, 1, General theory, *J. Fluid Mech., 12*, 481-500.

Hasselmann, K., 1966: Feynman diagrams and interaction rules of wave-wave scattering processes, *Rev. Geophys., 4*, 1-32.

Henyey, F.S., J. Wright, and S. M. Flatte, 1986: Energy and action flow through the internal wave field: an eikonal approach, *J. Geophys. Res., 91*, 8487-8495.

Holloway, G., 1980: Oceanic internal waves are not weak waves, *J. Phys. Oceanogr., 10*, 906-914.

Holloway, G., 1982: On the interaction time scales of oceanic internal waves, *J. Phys. Oceanogr., 13*, 293-296.

Kunze, E., 1985: Near-inertial wave propagation in geostrophic shear, *J. Phys. Oceanogr., 15*, 544-565.

Kunze, E., and P. Müller, 1989 The effect of internal waves on vertical geostrophic shear, in *Parameterization of Small-Scale Processes, Proceedings, 'Aha Huliko' a Hawaiian Winter Workshop*, edited by P. Müller and Diane Henderson, pp. 273-287, Hawaii Institute of Geophysics, Honolulu.

McComas, C. H., 1977: Equilibrium mechanisms within the oceanic internal wave field, *J. Phys. Oceanogr., 7*, 836-845.

McComas, C. H., and F. P. Bretherton, 1977: Resonant interaction of oceanic internal waves, *J. Geophys. Res., 83*, 1397-1412.

McComas, C. H., and P. Müller, 1981: Time scales of resonant interactions among oceanic internal waves, *J. Phys. Oceanogr., 11*, 139-147.

Müller, P., G. Holloway, F.S. Henyey, and N. Pomphrey, 1986: Nonlinear interactions among internal gravity waves, *Rev. Geophys., 24*, 493-536.

Olbers, D. J., 1976: Nonlinear energy transfer and the energy balance of the internal wave field in the deep ocean, *J. Fluid Mech., 74*, 375-399.

Olbers, D.J., 1981: The propagation of internal gravity waves in a geostrophic current, *J. Phys. Oceanogr., 11*, 1224-1233.

Pomphrey, N., J. D. Meiss and K. M. Watson, 1980: Description of nonlinear internal wave interactions using Langevin methods, *J. Geophys. Res., 85*, 1085-1094.

The WAMDI Group: Hasselmann, S., K. Hasselmann, E. Bauer, P. A. E. M. Janssen, G. J. Komen, L. Bertotti, P. Lionello, A. Guillaume, V. C. Cardone, J. A. Greenwood, M. Reistad, L. Zambresky, and J. A. Ewing, 1988: The WAM model -- a third generation ocean wave prediction model, *J. Phys. Oceanogr., 18*, 1775-1810.